

A Failed Cocrystallization Attempt Resulted in Novel First Polymorphic Structure: Crystal Structure and Hirshfeld Surface Analysis of the Polymorph of 4-Oxo-4-(pyridin-2-ylamino)butanoic Acid

G.K. RADHA^{1,*,}, MAHESHA^{2,}, S. NAVEEN^{3,*,}, N.K. LOKANATH^{2,} and P.A. SUCHETAN^{1,*,}

¹Department of Studies and Research in Chemistry, University College of Science, Tumkur University, Tumakuru-5761033, India

²Department of Studies in Physics, University of Mysore, Manasagangotri, Mysuru-570005, India

³Department of Physics, Faculty of Engineering and Technology, JAIN (Deemed-to-be University), Bengaluru-562112, India

*These authors contributed equally.

*Corresponding author: E-mail: pasuchetan@gmail.com

Received: 20 February 2023;

Accepted: 6 April 2023;

Published online: 28 April 2023;

AJC-21222

An attempt to cocrystallize 4-oxo-4-(pyridin-2-ylamino)butanoic acid (APS) with adipic acid in the ratio 1:1 was made. Solvent assisted grinding followed by solvent evaporation technique using ethanol as solvent yielded single crystals. Single crystal X-ray diffraction (SCXRD) studies of the obtained crystals showed that an attempt to obtain cocrystals has failed and instead has yielded a novel and very first polymorphic structure of APS (**1**). Compound **1** crystallizes with one molecule in the asymmetric unit in monoclinic $P2_1/n$ system, whereas, the earlier reported polymorph, **2**, crystallizes in triclinic $P-1$ system with two molecules in the asymmetric unit. The crystal structure of **1** features aminopyridine...carboxylic O-H...N and N-H...O=C interactions between molecules resulting in $R_2^2(8)$ supramolecular hetero-synthon, similar to that observed in polymorph **2**. The $R_2^2(8)$ dimer propagates into a 2D sheet along the body diagonal plane (intersecting a and c axis) via a pair of C-H...O intermolecular interactions having $R_2^2(14)$ motif. Polymorph **2**, on the other hand, features several C-H...O intermolecular interactions that extends the $R_2^2(8)$ supramolecular architecture into complex 1D columns. The Hirshfeld surface analyses including d_{norm} plots and two dimensional fingerprint analyses were conducted to confirm the presence of various hydrogen bonds/intermolecular interactions existing in the crystal structure of **1**. H...H contacts (dispersion interactions) contributes most to the Hirshfeld surface with a contribution of 40.8%, followed by O...H/H...O (28.4%), C...H/H...C (12.4%), N...H/H...N (9.3%) and others (9.1%). Further, the molecular structure, crystal structure and Hirshfeld surfaces including d_{norm} and fingerprint plots of **1**, **2** and a positional isomer 4-oxo-4-(pyridin-3-ylamino)butanoic acid (**3**) were compared to observe the similarities and differences in the three compounds.

Keywords: Cocrystals, Polymorph, X-ray diffraction, Hirshfeld surface, Hydrogen bonds.

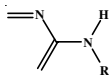
INTRODUCTION

Cocrystals are the solids that are crystalline single phase materials composed of two or more different molecular or ionic compounds generally in a stoichiometric ratio which are neither solvates nor simple salts [1]. The major application of cocrystals is in drug development. Cocrystals of Active Pharmaceutical Ingredients (APIs) with carefully selected coformers can improve the solubility (and hence better bioavailability) of the drug, either without altering or with not much modification in the structure or composition of the API (and hence not modifying its pharmacological action) [2]-an important and ideal criteria one expects a coformer to exhibit. Neat grinding or liquid/solvent

assisted grinding (LAG) followed by solvent evaporation method is a viable method to produce cocrystals as well as obtain their single crystals, which are suitable for single crystal X-ray diffraction studies [3]. However, there are a lot of challenges in designing cocrystals. Several considerations such as relative solubilities, structural relationships (complementary functional groups for forming hydrogen bonds), phase transitions, etc. of the two components have to be thoroughly understood prior to the design of a novel cocrystal [3]. An attempt to prepare cocrystals may not yield the desired results and one may end up with obtaining one of the starting components or an undesired ratio.

This is an open access journal, and articles are distributed under the terms of the Attribution 4.0 International (CC BY 4.0) License. This license lets others distribute, remix, tweak, and build upon your work, even commercially, as long as they credit the author for the original creation. You must give appropriate credit, provide a link to the license, and indicate if changes were made.

As a chemical crystallographic serendipity, an attempt to obtain cocrystals may sometimes lead to novel/undiscovered polymorphic structure of one of the components, which may otherwise not be observed or obtained by any well-known method of preparing polymorphs [4]. A cocrystal generally involves the hydrogen bonding between two components (*i.e.* hydrogen atom is shared between the hydrogen bond acceptor and donor) of which one is an acid and other is base. However, most of the times, mixing an acid and a base inevitably leads to salt formation, wherein, there is complete transfer of proton instead of the desired sharing. The ΔpK_a value is used a thumb rule to predict whether a given acid-base pair leads to a cocrystal or a salt [5]. Therefore, one of the strategies of preparing a cocrystal of a potential basic cofomer, which would otherwise form salts, is to reduce its basicity. For example, the cocrystallizing ability of 2-aminopyridine is explored by reducing its basic character (and thereby reducing its pK_a) by preparing its derivative *e.g.* 2-acetaminopyridine [6]. Therefore, it would be worthy to extend this idea to prepare similar molecules where in the basic character of 2-aminopyridine is reduced and hence the cocrystallizing ability is enhanced. One such example is 4-oxo-4-(pyridin-2-ylamino)butanoic acid [7] which is synthesized by treating 2-aminopyridine with succinic anhydride. In this molecule, the basic character of 2-aminopyridine is reduced due to the participation of adjacent amine group in amide formation. The molecule features several functionalities

such as amide, carboxylic acid and  through, which it can interact with functionalities such as amide, acid, *etc.* occurring in the other cocrystallizing component. Thus, it is possible to prepare cocrystals with variety of molecules bearing functionalities that differ both in nature and numbers. It is further observed that this compound is highly soluble in water [unpublished data] and thus could be an ideal cofomer candidate to prepare cocrystals of those APIs that have solubility issues [8]. In this regard, cocrystallization of 4-oxo-4-(pyridin-2-ylamino)butanoic acid with adipic acid was attempted. Liquid assisted grinding followed with solvent evaporation was used to prepare the desired cocrystal [3]. However, we ended up in obtaining a new polymorph of 4-oxo-4-(pyridin-2-ylamino)butanoic acid, which was subjected to single crystal diffraction studies and Hirshfeld surface analysis.

EXPERIMENTAL

4-Oxo-4-(pyridin-2-ylamino)butanoic acid was synthesized by the reported procedure [7]. The purity and structure of the compound were confirmed by various techniques such as melting point determination, Fourier transformed infrared spectroscopy (FT-IR), mass spectroscopy and ^1H & ^{13}C nuclear magnetic resonance (NMR).

Synthesis of cocrystal (rather an unsuccessful attempt): 4-Oxo-4-[(pyridin-2-yl)amino]butanoic acid (APS) (1 mmol) and adipic acid (1 mmol) were mechanically ground with few drops of ethanol by using mortar and pestle [9]. The mixture was further dissolved in ethanol (10 mL). It was heated to 60 °C and stirred continuously till the homogeneous solution was

formed and filtered. Upon slow evaporation, single crystals were obtained. Good quality single crystal suitable for SCXRD measurement was removed from the saturated solution and was subjected to SCXRD study.

X-ray crystallographic study: The X-ray intensity data were collected at 293 K on a Bruker Proteum2 CCD diffractometer equipped with an X-ray generator operating at 45 kV and 10 mA, using $\text{MoK}\alpha$ radiation of wavelength 0.71073 Å. Data were collected for 24 frames per set with different settings of φ (0° and 90°), keeping the scan width of 0.5°, exposure time of 5 s, the sample-to-detector distance of 45.10 mm and 2θ value at 54.96°. Image processing and data reduction were done using SAINT-Plus and XPREP [10]. Direct method available in SHELXS-97 [11] was employed to solve the structure. The first-difference Fourier map revealed the positions of all the non-hydrogen atoms, which were then anisotropically refined. All the hydrogen atoms were positioned geometrically. All carbon bound H atoms were positioned geometrically, with $C_{\text{aromatic}}\text{-H} = 0.93$ Å and $C_{\text{methylene}}\text{-H} = 0.97$ Å and refined using a riding model $U_{\text{iso}}(\text{H}) = 1.2U_{\text{eq}}(\text{C})$ for all carbon bound H atoms. The nitrogen and oxygen bound H atoms were also geometrically fixed, with $\text{N-H} = 0.86$ Å and $\text{O-H} = 0.82$ Å and refined using a riding model $U_{\text{iso}}(\text{H}) = 1.5U_{\text{eq}}(\text{N/O})$. All the geometrical calculations were carried out using the PLATON [12] program within the WinGX suite [13]. MERCURY [14] software was used to generate molecular and packing diagrams. Table-1 summarizes the crystallographic data and details of refinement parameters. Crystallographic data for the structures reported in this article is deposited with the Cambridge Crystallographic Data Centre with deposit no. CCDC-2206617; URL: <https://summary.ccdc.cam.ac.uk/structure-summary-form>.

TABLE-1
CRYSTAL DATA AND STRUCTURE
REFINEMENT PARAMETERS FOR 1

CCDC No.	2206617
Empirical formula	$\text{C}_9\text{H}_{10}\text{N}_2\text{O}_3$
Formula weight	194.19
Temperature/K	293(2)
Crystal system, space group	Monoclinic, $P2_1/n$
a (Å)	13.106(19)
b (Å)	5.088(7)
c (Å)	13.736(19)
β (°)	91.680(18)
Volume (Å ³)	916(2)
Z	4
ρ_{calc} (g/cm ³)	1.409
μ (mm ⁻¹)	0.108
F(000)	408.0
Crystal size (mm ³)	0.34 × 0.24 × 0.17
Radiation	$\text{MoK}\alpha$ ($\lambda = 0.71073$)
2θ range for data collection (°)	6.22 to 54.966
Index ranges	$-16 \leq h \leq 11$, $-6 \leq k \leq 6$, $-17 \leq l \leq 15$
Reflections collected	4753
Independent reflections	2080 [$R_{\text{int}} = 0.1499$, $R_{\text{sigma}} = 0.2017$]
Data/restraints/parameters	2080/0/128
Goodness-of-fit on F^2	1.077
Final R indexes [$I \geq 2\sigma(I)$]	$R_1 = 0.1578$, $wR_2 = 0.4077$
Final R indexes [all data]	$R_1 = 0.2841$, $wR_2 = 0.4676$
Largest diff. peak/hole/e Å ⁻³	0.34/-0.37

Hirshfeld surface calculations: Hirshfeld surface analyses were carried out and finger print plots were plotted using the CrystalExplorer 3.0 software [15]. The d_{norm} plots were mapped with colour scale in between -0.18 au (blue) and 1.4 au (red). The 2D fingerprint plots [16] were displayed by using the expanded view (0.6 - 2.8 Å) with the d_e and d_i distance scales displayed on the graph axes. When the cif. file of **1** was uploaded into the CrystalExplorer software, all bond lengths to hydrogen were automatically modified to typical standard neutron values *i.e.* C-H = 1.083 Å and N-H = 1.009 Å.

RESULTS AND DISCUSSION

Molecular structure of 1: The ORTEP diagram of **1** is shown in Fig. 1 and the selected bond lengths, bond angles and torsions are listed in Table-2. Compound **1** crystallizes in monoclinic crystal system $P2_1n$ space group with $Z = 4$ and one molecule in the asymmetric unit similar to that observed in the positional isomer **3** [17], while the reported polymorph **2** crystallizes in triclinic $P-1$ space group $Z = 4$ and two molecules (2A and 2B) in the asymmetric unit [7]. The cell parameters, cell volumes and unit cell densities in all the three are close to each other. The overlay of the molecular structure of **1** with 2A and 2B molecules (Fig. 2a-b) shows that the major difference in the molecular conformation is in the side chains-around ethylene C7 carbon atoms. On the other hand, the molecular conformation of **1** is nearly same as in **3** (Fig. 2c), with slight deviations observed around ethylene C8 carbon atom. In **1**, the side chain is bent at the C7 atom, similar to that observed in 2A, 2B and **3**, the dihedral angles between the C1-N2-C6(O1)-C7-C8 and the C8-C9-O2(O3) segment (C10-N4-C15(O4)-C16-C17 and the C17-C18-O5(O6) segment in 2B) being $86.71(1)^\circ$ in **1**, $79.79(2)^\circ$ in 2A, $81.57(2)^\circ$ in 2B and $76.67(2)^\circ$ in **3**. The pyridyl rings (C1-C2-C3-C4-C5-N1 in 1/2A/3 and C10/C11/C12/C13/C14/N3 in 2B) and the amide segments (-C1-N2-C6(O1)-C7- in 1/2A/3 and -/C10-N4-C15(O4)-C16- in 2B) in all the three compounds are nearly planar. The planarity is measured in terms of the dihedral angle between the pyridyl ring and the amide segment, which is $8.29(1)^\circ$ in **1**, $9.95(1)^\circ$ in 2A and $5.19(1)^\circ$ in 2B and $7.64(1)^\circ$ in **3**. The conformations of amide and carboxylic groups in **1** with respect to the central $-\text{CH}_2-\text{CH}_2-$ segment are similar to that observed in the symmetry independent molecules of the polymorphic structure *i.e.* molecules 2A and 2B and opposite to that seen in **3**. In **1**, 2A and 2B, the O-H of the carboxylic group is opposite to the $-\text{CH}_2-\text{CH}_2-$ segment of the side chain and, both carboxylic and amidic C=O bonds are anti to the H atoms of $-\text{CH}_2-$ groups to which they are attached. The carboxylic groups in the molecules of **1**, 2A and 2B assumes syn conformation with the C=O and O-H bonds pointing towards each other. However, in **3**, unlike **1**, 2A and 2B, the $-\text{COOH}$ group has anti-conformation with the C=O and O-H bonds pointing in opposite directions. Also, the O-H of the carboxylic group of **3** points towards the $-\text{CH}_2-\text{CH}_2-$ segment of the side chain, dissimilar to **1**, 2A and 2B. However, similar to **1**, 2A and 2B, both carboxylic and amidic C=O bonds in the positional isomer **3**, are *anti*- to the H-atoms of $-\text{CH}_2-$ groups to which they are attached. The molecular conformation of **1** is stabilized by an intramolecular

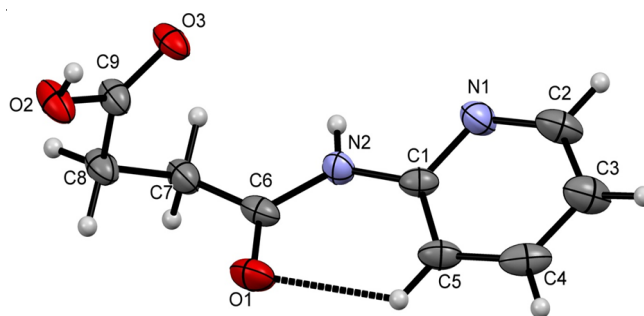


Fig. 1. ORTEP diagram of **1**. Displacement ellipsoids are drawn at the 30% probability level

TABLE-2
SELECTED BOND LENGTHS, BOND
ANGLES AND TORSIONAL ANGLES OF **1**

Bond	Length (Å)	Bond	Length (Å)
N2-C1	1.363(10)	C1-C5	1.388(12)
N2-C6	1.367(9)	C7-C6	1.491(13)
O3-C9	1.187(8)	C7-C8	1.523(11)
O2-C9	1.321(10)	C8-C9	1.500(11)
O1-C6	1.253(11)	C5-C4	1.402(13)
N1-C1	1.343(10)	C4-C3	1.367(13)
N1-C2	1.344(12)	C2-C3	1.387(15)
Bond	Angle (°)	Bond	Angle (°)
C1-N2-C6	130.8(8)	C9-C8-C7	111.5(6)
C1-N1-C2	117.3(8)	C1-C5-C4	118.3(8)
N2-C1-C5	124.8(8)	C3-C4-C5	121.8(9)
N1-C1-N2	113.5(7)	O3-C9-O2	122.4(7)
N1-C1-C5	121.6(8)	O3-C9-C8	123.1(8)
C6-C7-C8	112.5(9)	O2-C9-C8	114.5(6)
N2-C6-C7	116.9(8)	N1-C2-C3	126.2(9)
O1-C6-N2	121.8(9)	C4-C3-C2	114.8(10)
O1-C6-C7	121.3(8)	–	–
Bond	Torsion (°)	Bond	Torsion (°)
N2-C1-C5-C4	-178.9(7)	C6-N2-C1-N1	-171.8(7)
N1-C1-C5-C4	1.3(13)	C6-N2-C1-C5	8.5(14)
N1-C2-C3-C4	2.0(17)	C6-C7-C8-C9	62.2(10)
C1-N2-C6-O1	0.0(13)	C8-C7-C6-N2	-136.5(7)
C1-N2-C6-C7	179.0(7)	C8-C7-C6-O1	42.5(10)
C1-N1-C2-C3	-0.8(16)	C5-C4-C3-C2	-1.5(15)
C1-C5-C4-C3	0.0(14)	C2-N1-C1-N2	179.3(8)
C7-C8-C9-O3	17.4(14)	C2-N1-C1-C5	-0.9(13)
C7-C8-C9-O2	-164.0(8)	–	–

C5-H5...O1 hydrogen bond with a S(6) graph set motif similar to that observed in 2A and 2B molecules (Table-3).

TABLE-3
GEOMETRIC PARAMETERS FOR HYDROGEN-BONDS
AND OTHER INTERMOLECULAR CONTACTS (Å, °)
OPERATING IN THE CRYSTAL STRUCTURE OF **1**

D-H...A	D-H	H...A	D...A	D-H...A
O2-H3O...N1 ⁱ	0.82	1.92	2.6857	156
N2-H2N...O3 ⁱⁱ	0.86	2.00	2.8431	167
C4-H4...O1 ⁱⁱⁱ	0.93	2.54	3.3255	143
C5-H5...O1 [#]	0.93	2.33	2.8999	119

i: 1/2-x, 1/2+y, 1/2-z; ii: 1/2-x, -1/2+y, 1/2-z; iii: -x, 1-y, -z; #Intra

Crystal structure of 1: The supramolecular architectures in the crystal structure of **1**, **2** and **3** can be visualized as formed in two stages. In the crystal structure of **1**, in stage 1, the hetero

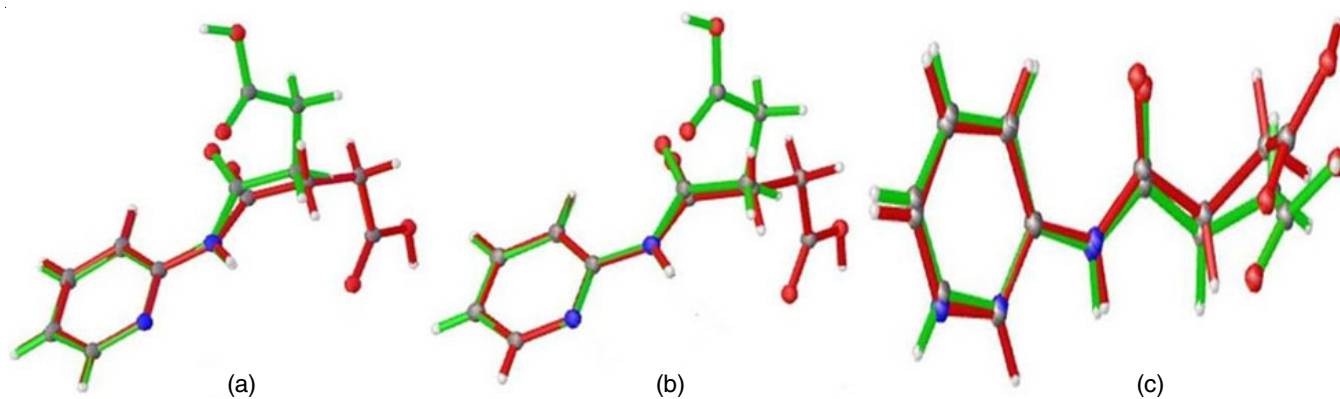


Fig. 2. An overlay diagram showing a view of the molecular fit of molecule 1 (green) and 2A (red) (a); molecule 1 (green) and 2B (red) (b); molecule 1 (green) and 3 (red) (c)

supramolecular synthon-prevalent in most of aminopyridine derivatives comprising a pair of $N-H_{amide} \cdots C=O_{carboxylic}$ and $O-H_{carboxylic} \cdots N_{pyridyl}$ moderate hydrogen bonds are observed. The $O2-H3O \cdots N1$ and $N2-H2N \cdots O3$ hydrogen bonds are observed in the crystal between the molecules related by two-fold roto-inversion axis constituting a hetero $R_2^2(8)$ synthon (Fig. 3). The synthon extends along b -axis to form a one dimensional column comprising $C_2^2(16)$ chains. Stage 1 in the crystal struc-

ture of **2** is somewhat similar with $N-H_{amide} \cdots C=O_{carboxylic}$ and $O-H_{carboxylic} \cdots N_{pyridyl}$ hydrogen bonds between symmetry independent molecules 2A and 2B generating a hetero $R_2^2(8)$ synthon propagating along crystallographic a -axis as one dimensional column [7]. The one dimensional column in **2** is further stabilized by a $C-H_{methylene} \cdots O=C_{carboxylic}$ intermolecular interactions between molecules 2A and 2B. In **3**, $C_1^1(10)$ chains formed by structure directing strong $O-H_{carboxylic} \cdots N_{pyridyl}$

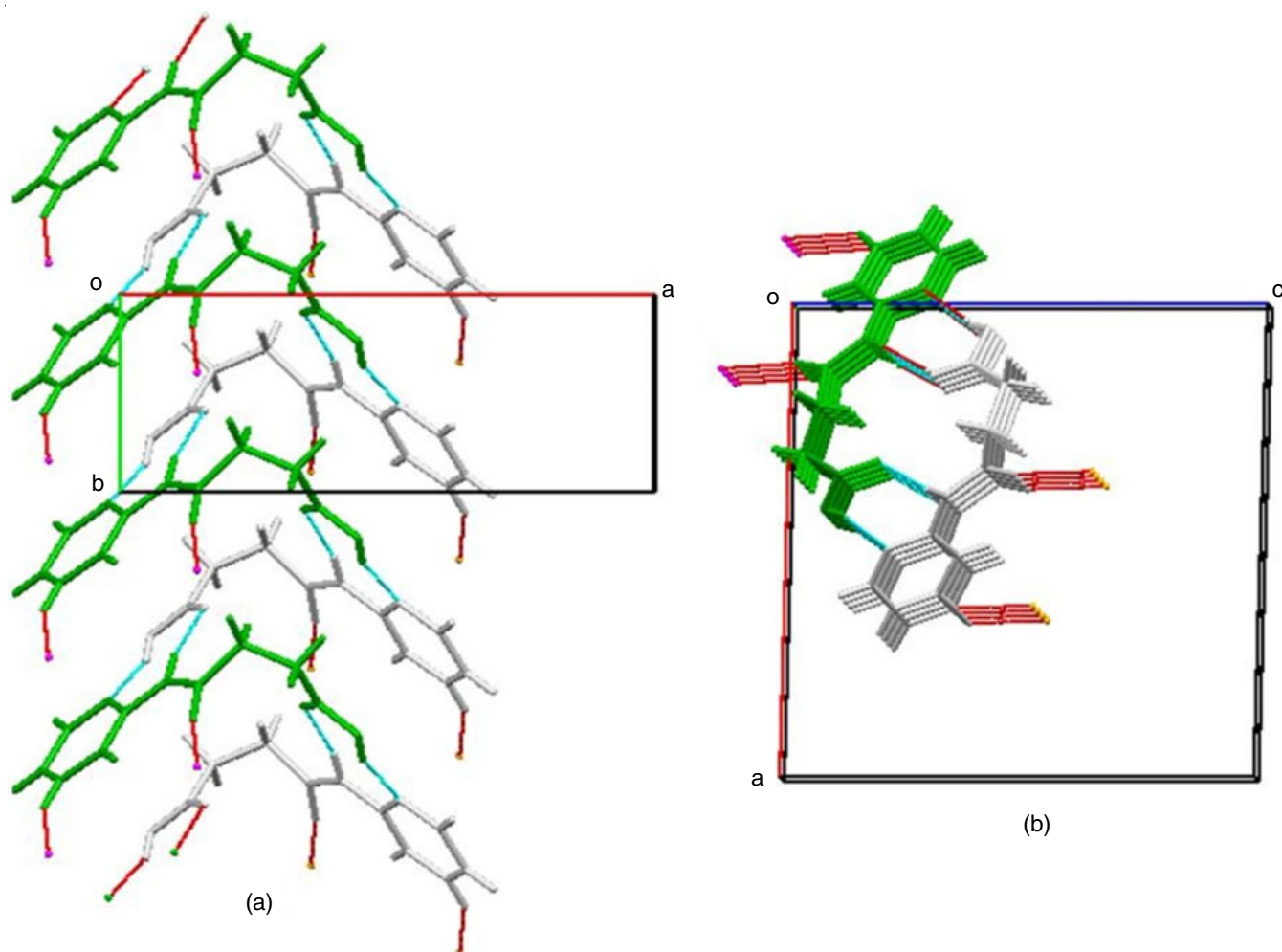


Fig. 3. (a) A partial view of the crystal packing in **1** when observed down the c -axis displaying one dimensional column along b axis; (b) A top view of the one dimensional columns along b -axis. Hydrogen bonds and intermolecular interactions are shown as thin blue lines

hydrogen bonds between the molecules are interlinked *via* C-H_{aromatic}...O=C_{amide} intermolecular interactions to form a chain-pair. These chain-pairs transform into a two dimensional zig-zag sheet in the *ab* plane *via* strong N-H_{amide}...C=O_{carboxylic} hydrogen bonded C₁(7) chains connecting the adjacent chain-pairs [17].

The stage 2 of supramolecular aggregation in crystals of **1** involves a pair of C4-H4...O1 intermolecular interactions having ring R₂²(14) motif between inversion-related molecules of the adjacent one dimensional columns, spreading into a two dimensional zig-zag sheet (Fig. 4). However, in **2**, in the second stage of aggregation, the adjacent columns are interlinked *via* a pair of C-H...O interactions leading into a one dimensional architecture and not a two dimensional sheet as in **1**. In **3**, a three dimensional supramolecular architecture is formed, wherein the two dimensional sheet obtained in the first stage is interconnected *via* a structure directing C₁(4) chain of C-H_{methylene}...O=C_{amide} intermolecular interactions along *b*-axis. Therefore, one can see some striking similarity and difference in the crystal structures of the two polymorphic structures and that of the positional isomer.

Hirshfeld surface analyses: Hirshfeld surface analysis of **1** including d_{norm} plots and two dimensional fingerprint plots were performed to explore qualitatively as well as quantitatively the contribution of various interatomic contacts to the Hirshfeld surface and to get further confirmation to the intermolecular interactions existing in the crystal. The presence of bright spots near O2, H3O, N1 and H2N atoms in the d_{norm} surface of **1** (Fig. 5a-b) confirms the participation of these atoms, as either donors or acceptors, in strong hydrogen bonding in crystal.

This is justifiable as moderate hydrogen bonds, namely, O2-H3O...N1 and N2-H2N...O3 exists in the crystal. Also, there are faint red spots near O1 and H4 atoms in the d_{norm} plots suggesting the involvement of these atoms in weaker intermolecular interactions. This supports the C4-H4...O1 intermolecular interactions present in the crystal. The ring/dimeric nature of the hydrogen bonded pairs O2-H3O...N1 and N2-H2N...O3 and C4-H4...O1 intermolecular interactions are depicted in the d_{norm} plots shown in Figs. 5a-b and 6a-c. Also, there are single red spots in the vicinity of each of the above mentioned atoms, thereby, suggesting the absence of bifurcated hydrogen bonds in the crystal. Fingerprint analyses of **1** (Fig. 5c-g) gives quantitative evidence to the various intermolecular interactions in the crystal structure. The highest contribution to the Hirshfeld surface is from dispersion interaction (H...H interactions), which contributes 40.8% to the surface. The next significant contribution is from O...H/H...O atomic contacts contributing 28.4% to the surface. The greater contribution from O...H/H...O is an evidence for the presence of N-H...O hydrogen bonds and C-H...O interactions in the crystal. The O...H/H...O atomic contacts appear as a pair of sharp spikes (Fig. 5d), suggesting strong nature of the O...H/H...O interaction and indicating the involvement of both -C=O and -OH groups of an acid group of a molecule (*i.e.* molecule acts as a hydrogen bond donor as well as an acceptor) in hydrogen bonding. The spikes appear at $d_i + d_e \sim 1.9$ Å, which is close to the H...A distance of 2.00 Å of the N2-H2N...O3 hydrogen bonds in the crystal (Table-3). The contribution of 9.3% to the Hirshfeld surface by N...H/H...N atomic contacts (Fig. 5e) is due to the N-H...N hydrogen bonds existing in the crystal. These contacts

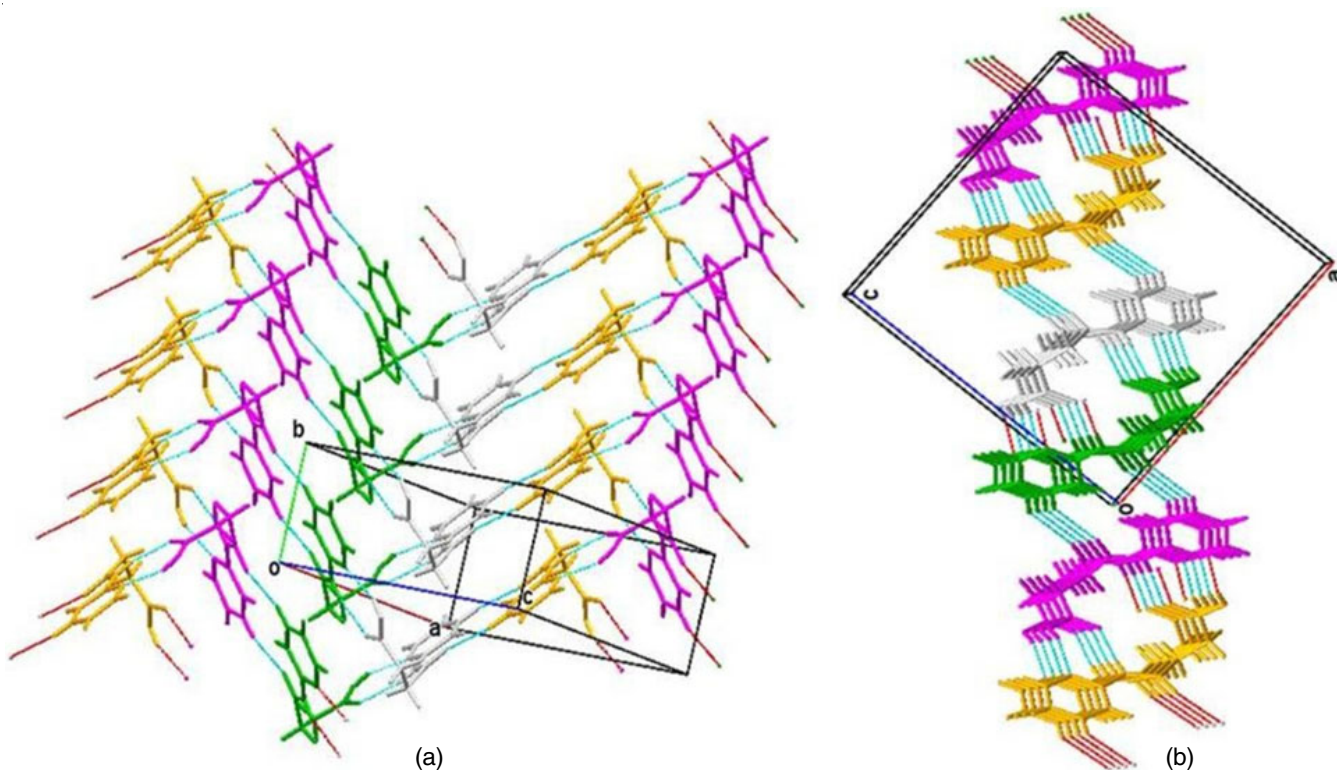


Fig. 4. Partial views (a and b) of the crystal packing in **1** displaying two dimensional zig-zag sheets. Hydrogen bonds and intermolecular interactions are shown as thin blue lines

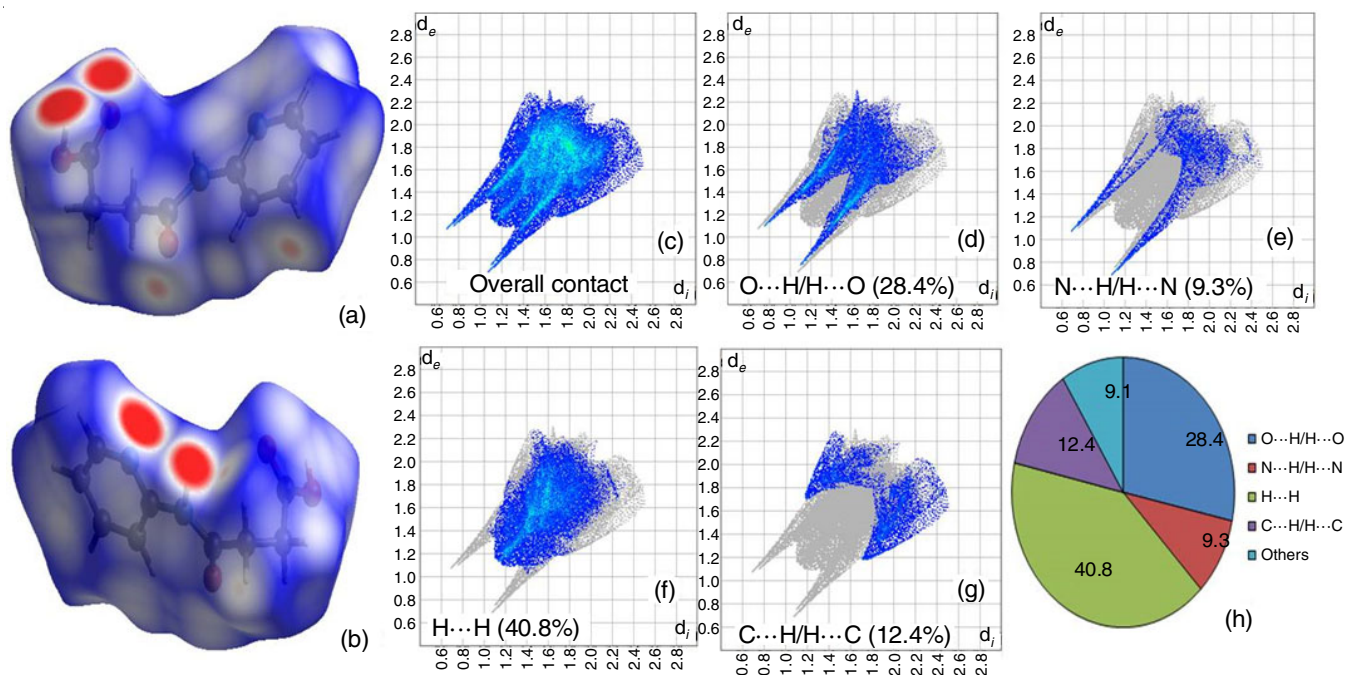


Fig. 5. Two different views of the d_{norm} plotted on Hirshfeld surface of **1** (a and b). Overall two dimensional FP of **1** (c) and FP's of individual atom...atom contacts: O...H/H...O (d), N...H/H...N (e), H...H (f) & C...H/H...C (g) and, comparison of different contacts contributing to the Hirshfeld surface (h)

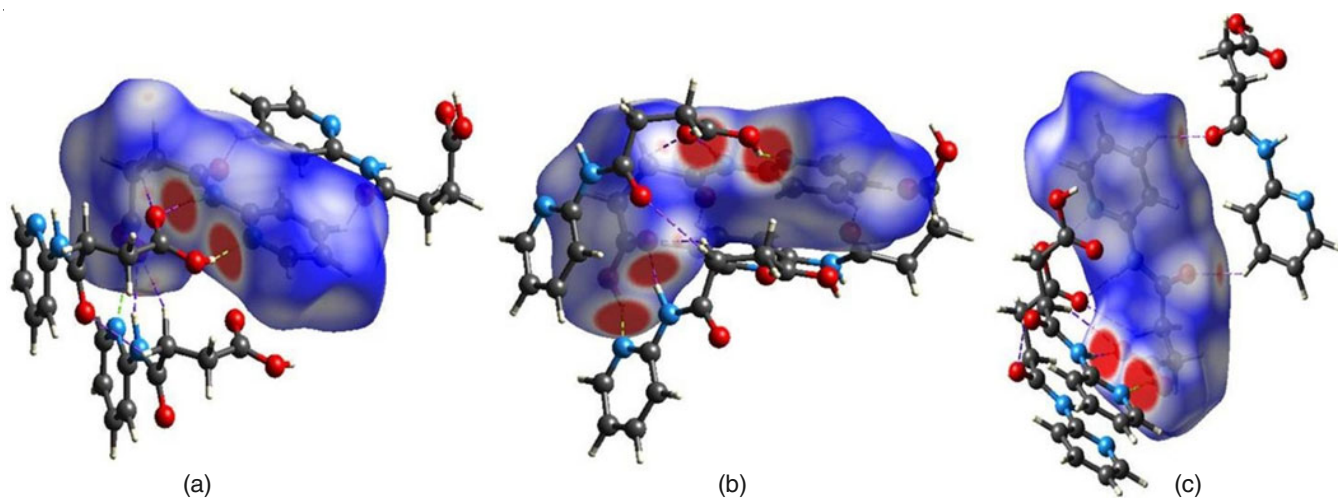


Fig. 6. d_{norm} plotted on Hirshfeld surface displaying evidence for $R_2^2(8)$ N-H...O and O-H...N hydrogen bonded hetero synthon (a) and C-H...O interactions- leading to dimeric homo synthon $R_2^2(14)$ -existing in the crystal structure of **1** (b)

appear as a pair of sharp spikes in the fingerprint suggesting the participation of both amide N-H and pyridine N-atom of each molecule in hydrogen bonding. Further, these spikes appear in the FP at $d_i + d_e \sim 1.8 \text{ \AA}$ which is very close to the H...A distance of 1.92 \AA of the O2-H3O...N1 hydrogen bonds in the crystal (Table-3). Though C...H/H...C atomic contacts contributes 12.4% to the Hirshfeld surface, there are no C-H... π interactions observed in the crystal. The contribution of different contacts to the Hirshfeld surfaces of 2A, 2B and 3 are H...H (38.9% in 2A, 41.7% in 2B and 34.4% in 3), O...H/H...O (30.4% in 2A, 27.1% in 2B and 31.4% in 3), N...H/H...N (9.9% in 2A, 9.2% in 2B and 11.7% in 3) and C...H/H...C (13.2% in 2A, 13.1% in 2B and 14.7% in 3) and are close to that observed

in that of **1**. Also, the shapes of d_{norm} surfaces and fingerprint of all **1**, 2A, 2B and **3** are similar with minor changes indicating similarities in the crystal structures of the three compounds.

Conclusion

The article describes the SC-XRD study and Hirshfeld surface analysis of a novel and the first polymorph of 4-oxo-4-(pyridin-2-ylamino)butanoic acid (**1**), which was obtained unexpectedly in attempt to prepare a cocrystal of 4-oxo-4-(pyridin-2-ylamino)butanoic acid with adipic acid in the ratio 1:1. A brief literature survey showed that such instances of obtaining unknown polymorphs of one of the components rather than a cocrystal is serendipitous and somewhat usual.

Solvent assisted grinding followed by solvent evaporation technique using ethanol as solvent yielded single crystals of **1**. The crystal structure of **1** features robust aminopyridine...carboxylic O-H...N and N-H...O=C interactions between molecules resulting in $R_2^2(8)$ supramolecular hetero-synthon, similar to that observed in the reported structure of **2**. The $R_2^2(8)$ dimer further propagates into a 2D sheet along the body diagonal plane (intersecting *a*- and *c*-axis) via a pair of C-H...O intermolecular interactions having $R_2^2(14)$ motif. Hirshfeld surface analyses including d_{norm} plots and two dimensional fingerprint analyses were conducted to confirm the presence of various hydrogen bonds/intermolecular interactions existing in the crystal structure of **1**. The H...H contacts contributes the most to the Hirshfeld surface (40.8%), followed by O...H/H...O (28.4%), C...H/H...C (12.4%), N...H/H...N (9.3%) and others (9.1%). Comparison of molecular structure, crystal structure and Hirshfeld surfaces including d_{norm} and FP plots of **1**, **2** and the positional isomer **3** indicated some striking similarities and differences in the three.

ACKNOWLEDGEMENTS

The authors are thankful to University of Mysore, Mysuru, India for providing the single-crystal X-ray diffraction facility.

CONFLICT OF INTEREST

The authors declare that there is no conflict of interests regarding the publication of this article.

REFERENCES

- S. Aitipamula, R. Banerjee, A.K. Bansal, K. Biradha, M.L. Cheney, A.R. Choudhury, G.R. Desiraju, A.G. Dikundwar, R. Dubey, N. Duggirala, P.P. Ghogale, S. Ghosh, P.K. Goswami, N.R. Goud, R.R.K.R. Jetti, P. Karpinski, P. Kaushik, D. Kumar, V. Kumar, B. Moulton, A. Mukherjee, G. Mukherjee, A.S. Myerson, V. Puri, A. Ramanan, T. Rajamannar, C.M. Reddy, N. Rodriguez-Hornedo, R.D. Rogers, T.N.G. Row, P. Sanphui, N. Shan, G. Shete, A. Singh, C.C. Sun, J.A. Swift, R. Thaimattam, T.S. Thakur, R.K. Thaper, S.P. Thomas, S. Tothadi, V.R. Vangala, D.R. Weyna, N. Variankaval, P. Vishweshwar and M.J. Zaworotko, *Cryst. Growth Des.*, **12**, 2147 (2012); <https://doi.org/10.1021/cg3002948>
- P. Vishweshwar, J.A. McMahon, J.A. Bis and M.J. Zaworotko, *J. Pharm. Sci.*, **95**, 499 (2006); <https://doi.org/10.1002/jps.20578>
- T. Frišèic and W. Jones, *Cryst. Growth Des.*, **9**, 1621 (2009); <https://doi.org/10.1021/cg800764n>
- M. Rafilovich and J. Bernstein, *J. Am. Chem. Soc.*, **128**, 12185 (2006); <https://doi.org/10.1021/ja063224b>
- S. Kumar and A. Nanda, *Mol. Cryst. Liq. Cryst.*, **667**, 54 (2018); <https://doi.org/10.1080/15421406.2019.1577462>
- C.B. Aakeroy, I. Hussain and J. Desper, *Cryst. Growth Des.*, **6**, 474 (2006); <https://doi.org/10.1021/cg050391z>
- P. Shet M, N. Shivalingegowda, S. Erachikkaiah, L.N. Krishnappagowda and P.A. Suchetan, *Chem. Data Coll.*, **13-14**, 113 (2018); <https://doi.org/10.1016/j.cdc.2018.02.002>
- S. Jagtap, C. Magdum, D. Jadge and R. Jagtap, *J. Pharm. Sci. Res.*, **10**, 2205 (2018).
- E. Krzyzak B. Szczesniak-Siega and W. Malinka, *J. Therm. Anal. Calorim.*, **115**, 793 (2014); <https://doi.org/10.1007/s10973-013-3185-1>
- Bruker APEX2, SAINT-Plus and SADABS. Bruker AXS Inc., Madison, Wisconsin, USA (2004).
- G.M. Sheldrick, *Acta Crystallogr. A*, **71**, 3 (2015); <https://doi.org/10.1107/S2053273314026370>
- A.L. Spek, *Acta Crystallogr.*, **A46**, c34 (1990); <https://doi.org/10.1107/S0108767390099780>
- L.J. Farrugia and G.X. Win, *J. Appl. Cryst.*, **45**, 849 (2012); <https://doi.org/10.1107/S0021889812029111>
- C.F. Macrae, I.J. Bruno, J.A. Chisholm, P.R. Edgington, P. McCabe, E. Pidcock, L. Rodriguez-Monge, R. Taylor, J. van de Streek and P.A. Wood, *J. Appl. Cryst.*, **41**, 466 (2008); <https://doi.org/10.1107/S0021889807067908>
- S.K. Wolff, D.J. Grimwood, J.J. McKinnon, D. Jayatilaka and M.A. Spackman, Crystal Explorer 3.0, University of Western Australia, Perth, Australia (2001).
- M.A. Spackman and J.J. McKinnon, *CrystEngComm*, **4**, 378 (2002); <https://doi.org/10.1039/B203191B>
- S. Naveen, E. Suresha, A.G. Sudha, N.K. Lokanath and P.A. Suchetan, *Chem. Data Coll.*, **5-6**, 79 (2016); <https://doi.org/10.1016/j.cdc.2016.11.002>